Article

Crystallogenesis Trends of Free and Liganded Aminoacyl-tRNA Synthetases

Richard Giege#, Elodie Touze#, Bernard Lorber, Anne The#obald-Dietrich, and Claude Sauter

Cryst. Growth Des., **2008**, 8 (12), 4297-4306 • Publication Date (Web): 11 November 2008

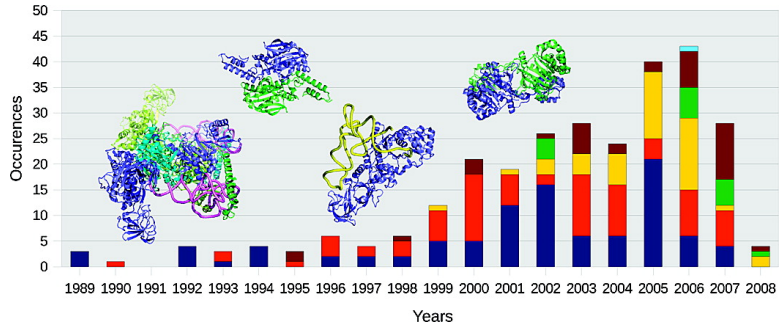

More About This Article

Additional resources and features associated with this article are available within the HTML version:

- Supporting Information
- Access to high resolution figures
- Links to articles and content related to this article
- Copyright permission to reproduce figures and/or text from this article

View the Full Text HTML

CRYSTAL GROWTH & DESIGN
2008
VOL. 8, NO. 12
4297–4306

Crystallogenesis Trends of Free and Liganded Aminoacyl-tRNA Synthetases†

Richard Giegé,* Elodie Touzé, Bernard Lorber, Anne Théobald-Dietrich, and Claude Sauter*

Architecture et Réactivité de l'ARN, Université Louis Pasteur de Strasbourg, CNRS, IBMC, 15 rue René Descartes, 67084 Strasbourg, France

Received July 18, 2008; Revised Manuscript Received September 29, 2008

Ⓦ **This paper contains enhanced objects available on the Internet at http://pubs.acs.org/crystal.**

ABSTRACT: Aminoacyl-tRNA synthetases (aaRSs) catalyze the attachment of amino acids on transfer RNAs (tRNAs) and thus enable the correct expression of the genetic code during protein synthesis. After a brief historical review of early aaRS crystallizations we present results of a survey of the crystallization conditions of 220 aaRSs (either free or bound to small ligands) and of 59 aaRS:tRNA complexes whose structures are hosted by the RCSB Protein Data Bank. These structures at resolutions between 4.5 and 1.2 Å are those of synthetases from the three kingdoms of life. Their phylogenic distribution is heterogeneous: most stem from bacteria and archaea and some from eukarya and organelles. Interesting correlations are found between biochemical, physical−chemical, and crystallographic parameters. They highlight common and more specific features of the crystallogenesis of free or liganded aaRSs. The effects of the chemical nature of the crystallant(s), of ligands and other additives, as well as of the presence of impurities and of the presence of flexible polypeptide domains on protein or protein/RNA crystallization are examined. Features that favor the growth of crystals diffracting X-rays at high resolution are discussed.

1. Introduction

Aminoacyl-tRNA synthetases (aaRSs) or aminoacyl-tRNA ligases (EC 6.1.1.x) occupy a central position in life by providing the interface between nucleotides and amino acids. They catalyze the attachment of amino acids on cognate transfer RNAs (tRNAs) and thus enable the correct expression of the genetic code via the codon−anticodon interactions tRNAs made with mRNAs during ribosome-dependent protein biosynthesis.[1] Following the usual nomenclature, each synthetase is named according to its specificity; for example, MetRS stands for methionyl-tRNA synthetase. Studies in solution have revealed that the aaRS family is very heterogeneous in terms of quaternary organization despite the fact that all its members have a similar biological function. Indeed, it is composed of monomers, dimers, or tetramers with a molecular mass ranging from 37 to 400 kDa.

Crystallization attempts on aaRSs began in the early 70s[2] and contributed to the birth of the science of biocrystallogenesis. Afterward, intensive research activity led to the resolution of a number of structures, especially in the frame of structural genomics projects. On 01 July 2008, the RCBS Protein Data Bank (PDB)[3] contained the atomic coordinates of 220 aaRSs (either in free form or associated to small ligands) and of 59 tRNA:aaRS complexes solved at resolutions ranging from 4.5 to 1.2 Å (Table 1). Besides the crystals that led to the above structures, many crystal forms that were of insufficient quality for structure determination have been reported (e.g., refs 4−6). At the end of the 80s, the first aaRS structures led to the unexpected discovery that this apparently ill-assorted collection of proteins can be arranged in two well-defined classes according to the topology of their active site. The synthetases of class I possess the well-known nucleotide binding domain called the Rossmann fold and those of class II a structural motif consisting of an antiparallel beta-sheet.[1]

Here we review how the first aaRSs were crystallized and how the studies on aaRSs have influenced and enriched the field of biocrystallogenesis. We then report the results of an analysis of the crystallization conditions that have led to published structures. Correlations between biochemical variables (such as purity, biological origin), physical−chemical variables (pH, crystallizing agents or crystallants, methods of crystal growth), and crystallographic parameters (space groups, resolution, solvent content) are presented. Trends in the aaRS crystallogenesis are commented on and practical considerations for the crystallization of free or liganded aaRSs are suggested, in particular to reach high resolution structures. Five well-characterized tRNA aminoacylation systems are described to illustrate the various topics.

2. Early Contributions to Bio-Crystallogenesis

Structural biology studies on aaRSs began in 1971 with the crystallization of an active fragment of *Escherichia coli* MetRS resulting from limited digestion of the entire protein with trypsin.[7] The first microcrystals were grown using the method of Jakoby.[8] The protein was sequentially salted-out in the cold at decreasing concentrations of ammonium sulfate, and subsequently the samples were equilibrated at a higher temperature. Afterward, larger crystals suitable for X-ray analysis were readily obtained by dialyzing a concentrated solution of the MetRS fragment against ammonium citrate in the cold.[7] From then on, it took about 30 years to get the definitive structures of the free MetRS and of that of the synthetase bound to methionine or to the catalytic intermediate methionyl-adenylate (see below).[9−11] MetRS crystals were soon followed by crystals of full-length LysRS from the yeast *Saccharomyces cerevisiae*[5] and of TyrRS from a thermophilic bacterium, *Bacillus stearothermophilus*.[12] Insurmountable difficulties were encountered with LysRS crystals that could never be improved, probably

† Part of the special issue (Vol 8, issue 12) on the 12th International Conference on the Crystallization of Biological Macromolecules, Cancun, Mexico, May 6−9, 2008.

* To whom correspondence should be addressed. (C.S.) E-mail: c.sauter@ibmc.u-strasbg.fr. Tel: 33 (0)3 88 41 71 02. Fax: 33 (0)3 88 60 22 18. (R.G.) Tel: 33 (0)3 88 41 70 58. Fax: 33 (0)3 88 60 22 18. E-mail: r.giege@ibmc.u-strasbg.fr.

10.1021/cg8007766 CCC: $40.75
Published on Web 11/11/2008

Table 1. Crystallographic Structures of aaRSs Deposited in the Protein Data Bank[a]

Class I aaRSs (157)

	Archaea (18)				Bacteria (112)					Eukarya (23)					Mitochondria & Virus (4)			
	Orig	apo	+ other	+ tRNA	*Orig*	apo	+ ade	+ other	+ tRNA	*Orig*	apo	+ ade	+ other	+ tRNA	*Orig*	apo	+ ade	+ tRNA
LeuRS (12)	*Pho*	-	1wkb	1wz2	*Eco* *Tth*	2ajg -	- - 1obc	2ajh 2aji 1obh 1h3n 2v0c	- - 2byt 2bte 2v0g									
IleRS (11)					*Sau* *Tth*	- 1udz 1wny	- 1wk8 1wnz 1jzq	- 1ile 1ue0 1jzs	1qu3 1qu2 1ffy -									
ValRS (5)					*Tth*	1iyw 1wka	1wk9 .	-	1ivs 1gax									
ArgRS (4)					*Tth*	1iqo	-	-	-	*Sce*	1bs2	-	-	1f7u 1f7v				
CysRS (3)					*Eco*	1li5 1li7	-	-	1u0b									
MetRS (19)	*Pab*	1mkh	1rqg	-	*Aae* *Eco* *Tth*	1pyb 1qqt 1f4l 1a8h 1woy 2d54 2d5b	- 1pfy 1pg0 - -	- 1p7p 1pfu 1pg2 1pfw 1pfv -	2csx 2ct8 - -	*Sce*	-	-	2hsn	-				
GluRS (16)					*Sel* *Tma* *Tth*	2cfo - 1gln	- - -	- 2o5r 1j09 1n75 2cuz	- - 1g59 1n77 1n78 2dxi 2cv1 2cv2 2cv0	*Sce*	2hrk 2hsm	-	2hra	-				
GlnRS (17)					*Dra* *Eco*	2hz7 1nyl	- -	- -	- 1gsg 1gts 1qrs 1qru 1qrt 1qtq 1euq 1euy 1exd 1o0b 1o0c 1zjw 1gtr 2rd2 2re8									
LysRS-1 (1)	*Pho*	1irx	-	-														
TyrRS (41)	*Afu* *Ape* *Mja* *Pho*	2cyb 2cya 1u7d 1u7x 2cyc	- - 1zh0 1zh6 2hgz 2ag6 2pxh 3d6v 3d6u -	- - 1j1u -	*Bst* *Eco* *Mtu* *Sau* *Tth*	4ts1 2ts1 1tyc 1tyb 1tya 1tyd 1x8x 1wq4 2jan - -	- 1vbm 1vbn - - -	3ts1 1wq3 2yxn - 1jij 1jil 1jik 1jii 1h3f	- - - - 1h3e	*Hsa* *Sce*	1n3l 1ntg -	1q11 -	- -	- - 2dlc	*Hsa* (M) *Ncr* (M) *Apo* (V)	- 1y42 2j5b	2pid	- 2rkj*
TrpRS (28)					*Bst* *Dra* *Mpn* *Tma* *Tth*	1d2r 1mb2 - 1yi8 2a4m 2yy5 - 2e17	1i6l 1i6m 1i6k - - - -	1m83 1mau 1maw 2ov4 1yia 1yid - 2g36 -	- - - 	*Hsa* *Sce*	1ulh 1o5t 2ip1	1r6u 1r6t 2quj -	2quh 2qui 2quk -	2azx 2ake 2dr2 -				

Class II aaRSs (122)

	Archaea (43)					Bacteria (69)					Eukarya (8)			Mitochondria (2)		
	Orig	apo	+ ade	+ other	+ tRNA	*Orig*	apo	+ ade	+ other	+ tRNA	*Orig*	apo	+ tRNA	*Orig*	apo	+ ade
SerRS (13)	*Mba* *Pho*	2cim 2cjb 2dq2	2cj9 2dq0	2cja 2dq1	- -	*Aae* *Tth*	- 1sry	2dq3 1ses 1set	- -	- 1ser				*Bta*	-	1wle
ThrRS (16)	*Pab*	1y2q 2hkz	2hl0 2hl1	2hl2	-	*Eco* *Sau*	1evk 1tje 1tke -	1evl 1fyf 1nyq	1tkg 1tky 1nyr	1qf6 1kog* -						
ProRS (16)	*Mja* *Mth*	1nj8 1nj2	- 1nj1 1nj5 1nj6	- -	- -	*Efa* *Eco* *Rpa* *Tth*	- 2dxa 2i4l 1h4t 1hc7	2j3l - 2i4m 2i4n -	2j3m - 2i4o -	- - - 1h4q 1h4s						
HisRS (9)	*Tac*	1wu7	-	-	-	*Sau* *Eco* *Tth*	1qe0 1kmn 1adj 1h4y	- 1kmm 1ady	- 2el9 1htt -	- - -						
GlyRS (8)						*Tma* *Tth*	1j5w 1ati	- 1ggm	- 1b76	- -	*Hsa*	2pme 2pmf 2q5h 2q5i				
AspRS (12)	*Pko* *Sto*	- -	- -	1b8a 1wyd	- -	*Eco* *Tth*	1eqr 1n9w 1low	- 1g51	- -	1c0a 1il2 1efw	*Sce*	1eov	1asy 1asz			
AsnRS (4)	*Pho* *Pfu*	1x56 1nnh	1x55 -	1x54 -	- -											
LysRS (8)						*Eco*	1lyl 1bbu 1bbw 1e1o	1e1t	1e22 1e24	-	*Hsa*	3bju	-			
AlaRS (10)	*Pho*	1v7o 1v4p 2e1b 1wxo	-	1wnu	-	*Aae*	1riq 1yfs 1yft 1ygb	-	1yfr	-						
PheRS (13)	*Pho*	2cxi	-	-	-	*Sha* *Tth*	- 1pys	- 1b7y 1jjc 2aly	2rhq 2rhs 2akw 2amc 1b70	- 1eiy 2iy5				*Hsa*	3cmq	-
PylRS (7)	*Mma*	2q7e 2e3c	2zim 2zce	2q7g 2q7h 2zcd												
SepRS (6)	*Afu* *Mja* *Mma*	- 2du7 2odr	- - -	- - -	2du3 2du4 2du5 2du6 - -											

[a] Synthetases are listed according to their class and subclass ranking (a in orange, b in yellow and c in pink), and their phylogenic origin in the three kingdoms of life, that is, archaea (A), bacteria (B), and eukarya (E) with a distinction for mitochondria (M) and viruses (V). Abbreviations used for organism names are as follows: (A) *Ape*, *Aeropyrum pernix*; *Afu*, *Archaeoglobus fulgidus*; *Mja*, *Methanocaldococcus jannaschii*; *Mba*, *Methanosarcina barkeri*; *Mma*, *Methanosarcina mazei*; *Mth*, *Methanothermobacter thermoautotrophycum*; *Pab*, *Pyrococcus abyssi*; *Pfu*, *Pyrococcus furiosus*; *Pho*, *Pyrococcus horikoshii*; *Pko*, *Pyrococcus kodakaraensis*; *Sto*, *Sulfolobus tokodaii*; *Tac*, *Thermoplasma acidophylum*; (B) *Aae*, *Aquifex aeolicus*; *Bst*, *Bacillus stearothermophilus*; *Dra*, *Deinococcus radiodurans*; *Eco*, *Escherichia coli*; *Efa*, *Enterococcus faecalis*; *Mtu*, *Mycobacterium tuberculosis*; *Rpa*, *Rhodopseudomonas palustris*; *Sau*, *Staphylococcus aureus*; *Sha*, *Staphylococcus haemolyticus*; *Sel*, *Synechococcus elongatus*; *Tma*, *Thermotoga maritima*; *Tth*, *Thermus thermophilus*; (E+M) *Bta*, *Bos taurus*; *Ncr*, *Neurospora crassa*; *Hsa*, *Homo sapiens*; *Sce*, *Saccharomyces cerevisiae* and (V) *Apo*, *Acanthamoeba polyphaga* for the amoeba harboring the Mimivirus. AaRS structures are designated by their PDB accession code and divided in four groups: (i) column "apo" for apoproteins (including structures with bound metal ions), (ii) column "+ ade" for complexes with adenylates or adenylate analogs, (iii) column "+ other" for complexes with any other small ligands, such as amino acids, ATP, and their combinations, and (iv) column "+ tRNA" for aaRS:tRNA complexes with or without small ligands; (*) indicates a complex with a mRNA fragment instead of tRNA. Underlined accession codes correspond to structures displayed in Figure 2. In the web version of this table, each accession code is provided as a clickable hyperlink to the corresponding PDB entry.

because of the presence of structural heterogeneities in this eukaryal protein. Later this appeared to be not exceptional at all: crystals with limited diffraction hampered the structure determination of several native eukaryal aaRSs. In the case of yeast AspRS,[13,14] disorder in the lattice was caused by the presence of a flexible N-terminal extension.

2.1. Introduction of New Crystallization Approaches. Structural investigations on aaRSs have rapidly led to the implementation of new crystallization approaches. LysRS and TyrRS crystallizations were run in dedicated microdialysis cells (Cambridge Buttons) that had been initially developed for TyrRS and are still in use today. Modern designs include the double-dialysis setup[15] and the Microdialysis Rod.[16] On the other hand, the better crystallizability of TyrRS isolated from heat-loving bacilli with respect to that of the enzyme from mesophilic *E. coli*, was a key finding for the progress of structural biology. It is now recognized that the lesser conformational flexibility of temperature-resistant proteins favors crystallization. This triggered the rush for systematic crystallization assays with proteins from thermophiles and more generally from organisms living under extreme conditions.[17] As a consequence, 57% of the aaRSs listed today in the PDB come from extremophiles (Table 1 and, for example, refs 18−22).

Dimeric TrpRS attracted the attention of molecular biologists because of its small size (subunit M_r 37 kDa),[23] its peculiar enzymological and immunochemical properties,[24] and its resemblance with TyrRS.[25] Although TrpRS was among the first to be crystallized[26,27] the determination of its structure was delayed because its crystals had growth defects and were polymorphous.[28,29] In 1978, long before sparse matrix screening had become a common practice,[30] C. W. Carter Jr. introduced statistical methods (such as incomplete- or later full-factorial and response-surface analysis) to attempt to overcome these difficulties. By analyzing the positive, neutral, or negative contribution of every ingredient of the crystallization medium it was possible to find new crystal forms and optimize crystallization conditions.[4,29,31] This approach was determining for the preparation of crystals of *B. stearothermophilus* TrpRS with superior diffraction properties.[32]

2.2. Stabilization of aaRS:tRNA Complexes. The 3D structure of an aaRS:tRNA complex was a long pursued dream, the major obstacle being the belief that such entities are not stable at the high salt concentrations required for crystallization. For these reasons, the very first crystallization conditions were searched in strictly nonionic crystallants. The breakthrough occurred in 1980 when it was realized that the rationale underlying the crystallization of complexes was wrong. Indeed, it was demonstrated that the association between aaRSs and tRNAs as well as the aminoacylation activities are maintained above 1.0 M ammonium sulfate.[33−36] The effect appears to be specific to ammonium sulfate since this salt sustains strong protein/RNA interactions at high concentration although (similar to other salts) it disrupts ionic bonds at low concentration. This remarkable property opened the way to the crystallization of the AspRS/tRNA^{Asp} complex[33] and of many other protein/RNA complexes.[37] The first structures solved were those of the *E. coli* Gln[38] and *S. cerevisiae* Asp[39] systems. Statistics confirm that ammonium sulfate is an excellent crystallant for aaRSs (see below).

2.3. The Concepts of Purity and Homogeneity. Crystallogenesis studies on aaRSs and on tRNAs have highlighted the importance of the parameter *purity*. In 1986, the key role of the absence of impurities for macromolecular crystal growth was demonstrated for the first time.[40] Although crystallization is a purification technique[41] in the case of macromolecules[42] like in that of small molecules, most contaminated samples yield crystals with growth defects and limited diffraction power. In other words, in structural biology purity not only means the absence of unrelated macromolecules or of undesired small molecules, but it also includes the absence of chemical or of conformational heterogeneities. In the past, these criteria have not often been fulfilled especially when working with aaRSs. For instance, partial proteolysis of the N-terminal extension of *S. cerevisiae* AspRS does not prevent its crystallization as a free enzyme[6] or as a complex with tRNA,[35,43] but crystals of the apoprotein are of mediocre diffraction quality and crystals of the complex suffer from structural disorder. Indeed, the N-terminus is not visible in the electron density map of the AspRS/tRNA^{Asp} complex because it is floppy in the crystals.[39] It also interferes with a packing contact in the crystals of the apo-AspRS. Better crystals that are suitable for structure determination can only be produced when this eukaryotic specific domain is deleted.[13,14,44] Similarly, the best crystals of bacterial AspRSs grow only when minute contaminants that exhibit some sequence similarity are removed.[45] These observations should urge crystal growers to probe macromolecular samples for purity and homogeneity with appropriate analytical tools.[46] Under prenucleation conditions impurities and heterogeneities frequently induce aggregation. Dynamic light scattering (DLS) measurements may be a good indicator of the quality of the samples as was shown in the cases of yeast AspRS,[47] *E. coli* aaRSs (Asn-, Leu-, ValRS),[48] and *B. stearothermophilus* TrpRS.[29]

Finally, this concept of "crystallography grade purity" has led to the systematic use of additives that stabilize aaRSs during the stages of purification. For instance, EDTA is used to remove contaminating heavy metal ions, DTE, DTT or mercaptoethanol to prevent oxidation, protease inhibitor cocktails (containing PMSF, AEBSF, pepstatin, bestatin, etc...) to prevent proteolysis and ensure protein integrity, and minute concentrations of toluene or sodium azide to hinder bacterial growth during crystallization.[46]

3. The Family of Aminoacyl-tRNA Synthetases

3.1. General Considerations. The increasing number of structures deposited with the PDB shows that the structural biology of aaRSs is flourishing (Figure 1). As much as 77% of the sets of atomic coordinates were actually deposited within the last 10 years. So far, the distribution of the synthetases from the three kingdoms of life is uneven: the bacterial proteins represent the majority (65%), followed by those from archaea (22%) and eukarya (13%) (Figure 1). The aaRS of higher eukaryotes are rare (6%) and those of organelles are almost unexplored (1.5%). Figure 2 displays representative structures of all types of aaRSs (at present not all are available for the same organism). In total 16 aaRS/tRNA complexes of different specificities are known; those specific for Ala, Asn, Gly, His, and Lys are still missing. The list also comprises the structures of a viral aaRS[49] and of a mitochondrial aaRS interacting with a group I intron RNA.[50] Three atypical aaRSs were recently discovered. They are the class I LysRS[51] (a protein showing striking structural similarity with bacterial class I GluRS and replacing canonical class II LysRS in the archaea where this aaRS is absent), the class II PylRS[52−54] (a synthetase charging the 22nd amino acid pyrrolysine or Pyl on a specialized tRNA in a few archaea), and the class II SepRS[55,56] (a protein present in several methanogenic archaea lacking CysRS, that charges

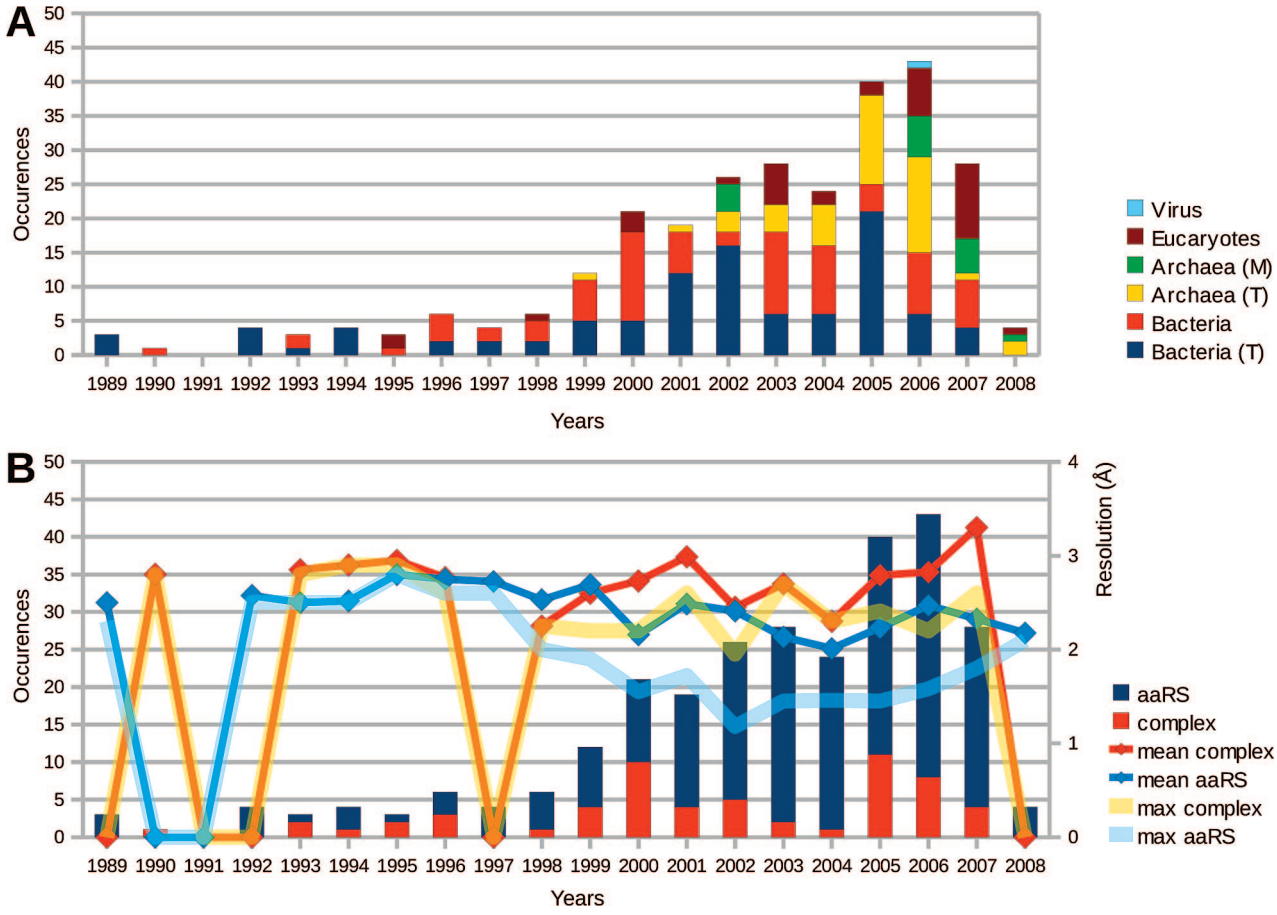

Figure 1. Aminoacyl-tRNA synthetases in the PDB. (A) Biological source of aaRSs; extremophiles are indicated by a letter: T for (hyper)thermophiles and M for methanogenes. (B) Distribution of PDB contribution (free aaRSs and complexes) over the years. Broken lines indicate the evolution of the resolution for both categories of structures with the average value and the maximum achieved for the corresponding year.

phosphoserine or Sep on $tRNA^{Cys}$, the latter being subsequently converted into cysteinyl-$tRNA^{Cys}$ by another enzyme).

3.2. Aminoacylation Systems at a Glance. The aaRSs specific for Asp, Met, Phe, Trp, and Tyr were most thoroughly investigated over the last 40 years and deserve particular attention. They cover about 40% of known aaRS structures, were among the first to be crystallized and the structures of some free tRNAs[57,58] are also known. They give a taste of how diverse protein architectures can be in a single group of ubiquitous enzymes.

So far, TyrRSs are by far the most studied with 41 structures. As mentioned above crystallographic data on *B. stearothermophilus* apo-TyrRS released in 1976[59] led to the discovery of a Rossmann fold[60] in the catalytic site. In all crystal structures of native TyrRSs,[61] there is no well-defined electron density for the C-terminal tRNA-binding domain. This part of the polypeptide chain clearly hinders the formation of an ordered packing. It was resected in all mini-TyrRSs crystallized up to now.[62] TyrRS serves as a model enzyme to investigate the expansion of the genetic code. Therefore, TyrRS mutants were designed, crystallized and their structure solved to engineer an enzyme able to activate artificial amino acids, such as 3-iodo- or O-methyl-L-tyrosine, and subsequently to incorporate them into proteins (e.g., refs 63 and 64).

TrpRSs (28 structures solved) are closely related to TyrRSs. Both are small dimeric class Ic synthetases with structural homologies (Figure 2). Half of the TrpRS structures are of human origin[65−70] including three heterologous complexes of human TrpRS (either full-length or N-terminally truncated forms) with the closely related bovine $tRNA^{Trp}$ transcript produced by in vitro transcription.[68,69] These complexes were crystallized under close conditions in 2 M ammonium sulfate solution at neutral pH and at 4 °C.

The crystallogenesis and crystallography of MetRSs has encountered many difficulties. Some of them could be overcome by cleaving off a part of the protein.[7] Most of the 19 structures were released only recently. Despite their functional uniqueness, these enzymes show an unexpected structural variability since they can be either monomeric or dimeric depending on their origin. Further, dimeric ones can be transformed in active monomers by truncating of their C-terminal domain.[71] The knowledge accumulated over years has provided clues about how to tailor the structure of these enzymes, to improve their crystal growth (in particular by adding an analog of their substrate to stabilize their structure)[29,72−74] and so to facilitate crystal production. Similar observations were made on a great variety of proteins and, as a consequence, protein engineering has become a general trend in the field.[75]

AspRSs (12 structures) are the only synthetases for which structures of a free aaRS,[6,44] a free tRNA,[76,77] and an aaRS/tRNA complex[33,39] are known from a same organism (the yeast *S. cerevisiae*). AspRSs from various sources have been crystallized as well as heterologous complexes made of bacterial enzymes bound to yeast tRNA.[78,79] Their structures highlight the modular nature of aaRSs and give an insight in the evolution of this protein family. Figure 3 compares the 3D structures of AspRSs from the three kingdoms of life. The homodimeric quaternary structure is conserved with each monomer divided

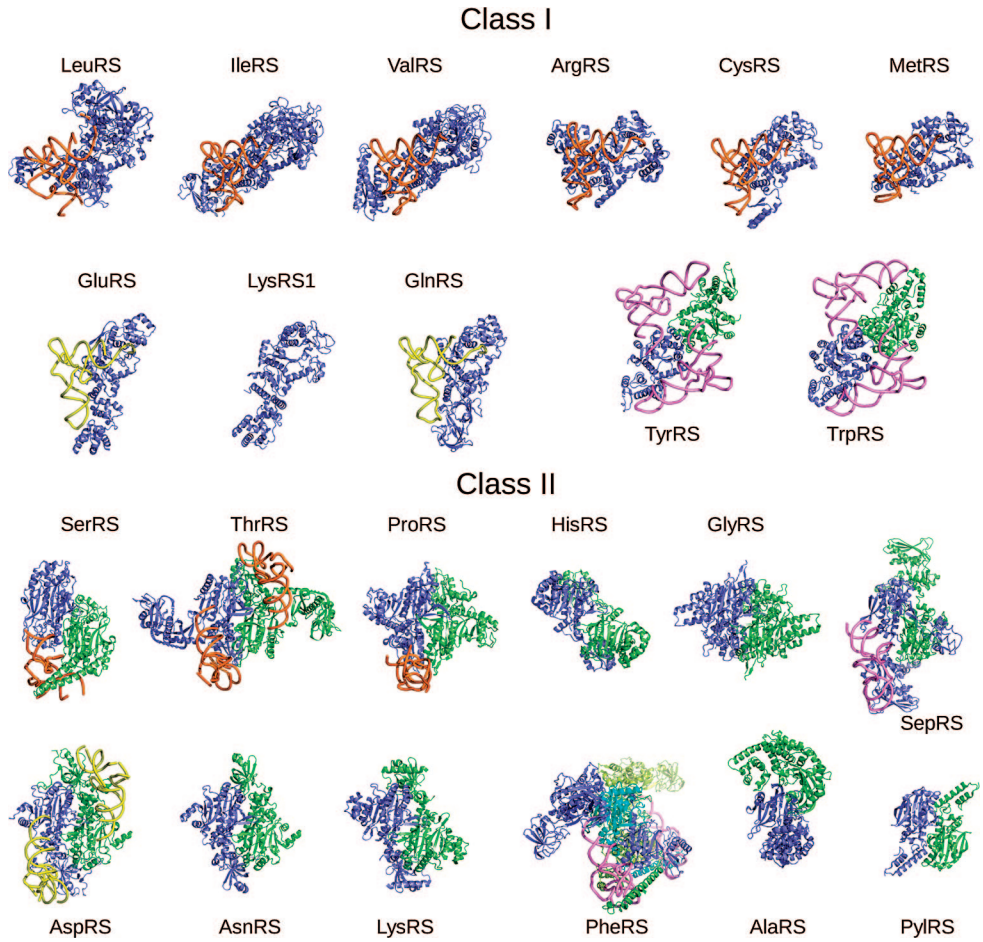

Figure 2. Gallery of aaRS structures. Aminoacyl-tRNA synthetases from class I and II are displayed in the top and bottom panel, respectively. Subclass distribution is indicated by tRNA colors with orange, yellow, pink backbones for subclass a, b, c, respectively. AaRSs in each class are displayed with their catalytic domain in the same orientation. The second subunit of dimers ($\alpha 2$) is shown in green. It the case of the tetrameric PheRS ($\alpha 2\beta 2$), one heterodimer ($\alpha\beta$) is shown in blue and the other is shown in green. The PDB accession codes of the structures shown here are underlined in Table 1. This figure, as well as Figure 3, was prepared with Pymol (DeLano Scientific LLC - www.pymol.org).

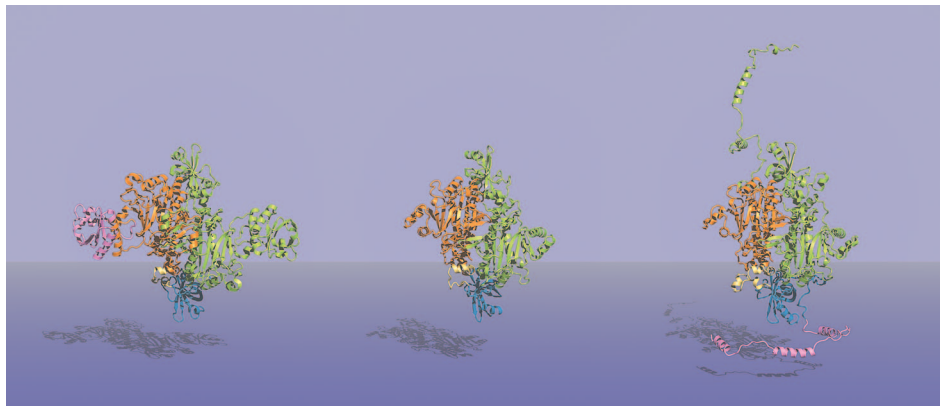

Figure 3. An example of structural variability of aaRSs during evolution: the case of AspRSs. This figure shows the organization of homodimeric AspRSs in the three kingdoms of life. From the left to the right, bacterial- (*T. thermophilus*), archaeal- (*P. horikoshii*) and eukaryal-type (*S. cerevisiae*) aaRSs are displayed with their anticodon binding domain in blue, connecting or hinge region in yellow and catalytic domain in orange colors. The second monomer is indicated in light green and kingdom specific extensions are in pink colors. The exact fold of the N-terminal extension of yeast AspRS is unknown and the present model is based on structure predictions.[80]

in an anticodon-binding domain, a hinge region, and a catalytic domain. Besides these common features, the archaeal AspRS is the most compact and the bacterial protein contains a specific insertion in its catalytic domain. The eukaryal enzyme is characterized by the presence of an N-terminal extension which ensures additional functions including the enhancement of tRNA binding.[80] The latter is also involved in the regulation of the expression of the protein and in its association in multienzymatic complexes (reviewed in ref 1). The supplementary functions vary from one organism to another. As reported above, the presence of such extensions can have deleterious effects on crystallization.

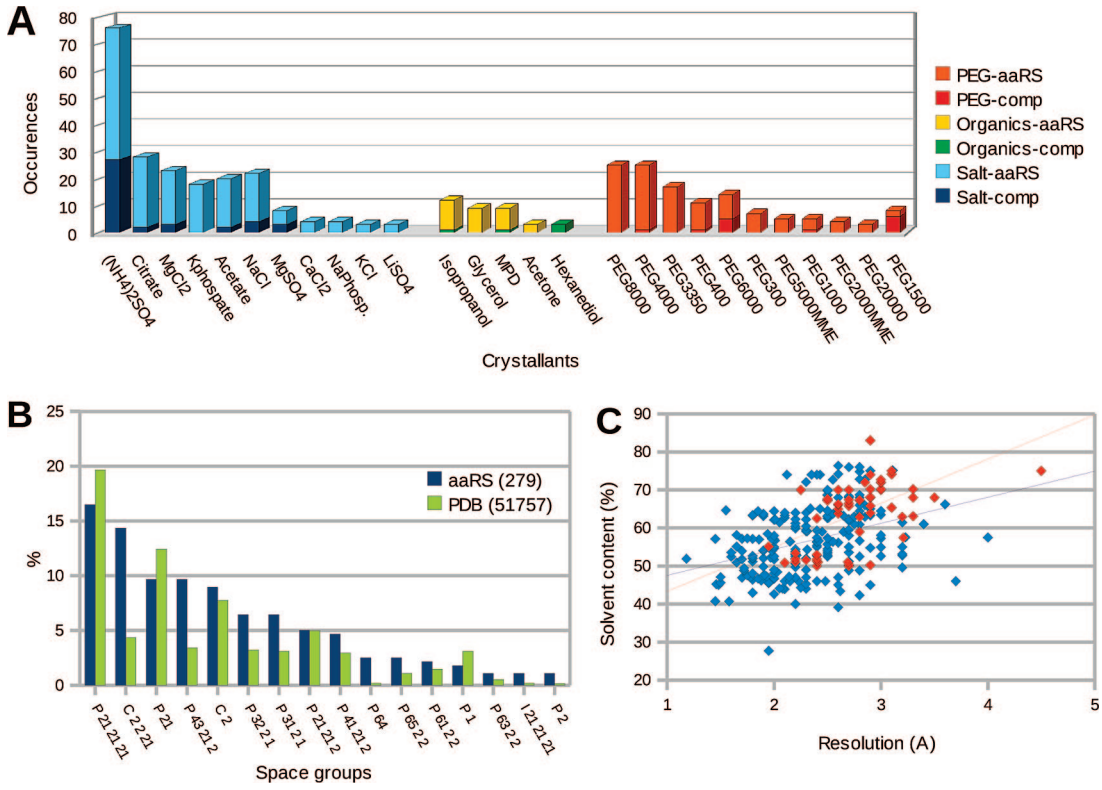

Figure 4. Crystallization of aminoacyl-tRNA synthetases. (A) Occurrence of crystallants (salts, organics and PEG) in crystallizations of free aaRSs or in complex with tRNA ("aaRS" or "comp", respectively). For a given structure, a crystallant can be a single chemical compound or a combination of two or more compounds (see text). (B) Space group distribution as compared to the overall distribution in the PDB (as of July 1, 2008). (C) Solvent content of free aaRS (blue diamonds) and aaRS/tRNA (red diamonds) crystals as a function of resolution with corresponding regression lines ($R^2 = 0.31$ and 0.13, respectively) depicted in similar colors.

Structural information on PheRSs (with 13 structures) comes from crystals of free PheRS[18,81] and of PheRS/tRNA^{Phe} complexes.[19,82] It was obtained relatively recently due to the large size, the tetrameric organization, and the conformational heterogeneity of the enzymes. It should not be forgotten that the characteristic L-shape fold common to tRNAs was discovered in 1973 owing to the crystallographic structure of tRNA^{Phe}.[83] Today, PheRS structures are known from five organisms, including *Homo sapiens.* The last addition is the human mitochondrial synthetase.[84]

3.3. Aminoacyl-tRNA Synthetases in the PDB. In order to compare different aspects of the structural investigations on aaRSs, from crystallization to final 3D model, a set of indicators was extracted from PDB using basic scripts and represented as histograms.

Crystallization. Information about the chemical nature of the crystallant(s), the pH and crystallization methods was collected from the line of comment REMARK 280 of each entry. At this stage, our analysis is partial since crystallization data for 12% of the structures are not documented at all, 10% are restricted to the pH value, and many entries lack details (such as concentration values and units, volumes, methods, droplet mixing ratio...) without which crystallization cannot be reproduced. In spite of this, well-documented entries suggest a few general trends. Although the crystallization method is not indicated in 23% of the cases, vapor diffusion is by far the preferred one with 70% of the entries. The use of dialysis, microbatch, evaporation or liquid−liquid diffusion remain anecdotal with 3, 2, 1 and 1% of the entries, respectively. Albeit the description of the crystallization cocktail is usually very brief, among the 79% of the exploitable data, crystallization is achieved in a majority by combining two crystallants, or using a single one or a mixture of 3 to 4 (41, 25, and 12%, respectively). Ammonium sulfate appears in more than a quarter of the entries and is the most effective crystallant for these RNA binding proteins, not only before but also after the popularization of commercial sparse matrices (69 entries since 2000 on 76 occurrences) (Figure 4A). For aaRS/tRNA complexes, this salt is present in 56% of the entries for which the composition of the crystallization medium is indicated.

Additives used in crystallization also reveal specific features. AaRS catalyze tRNA aminoacylation in a two-step reaction, the first one consisting in the activation of the amino acid by ATP to form an intermediate called aminoacyl-adenylate.[1] Among about 120 small molecules (listed as "other" and "ade" in Table 1) and besides the 20 amino acids observed in aaRS structures, more than 25% are natural adenylates or chemically stable analogues. The latter are primarily added to stabilize the conformation of the active site and to study the catalytic pathway.[29,72−74]

Information on the pH of the crystallization medium is available for nearly all entries. The pH ranges from 4.5 to 9.5, which corresponds to the range covered by commercial screens. Let us recall that in the absence of a sufficient concentration of buffering substance, the pH in droplets equilibrated by vapor diffusion is governed by the pH of the reservoir when the crystallant is ammonium sulfate.[85,86] Recently, we have noticed that there are organism-to-organism variations in the pI of aaRSs.[87] A deeper analysis of the data in the PDB will involve the search of a correlation between the pH and the pI of the proteins. As pointed by other crystal growers, well-documented crystallization data are crucial for statistical analyzes. One payback of the effort may be the design of oriented sparse matrices.[88,89]

Table 2. How aaRSs and tRNAs Contributed to Improve Biocrystallogenesis Strategies[a]

needs	methodological and technical improvements
miniaturization of crystallization assays	implementation of dedicated setups (microdialysis, vapor diffusion)
stabilization of tRNA:aaRS complexes by ammonium sulfate	crystallization possible
absence of macromolecular impurities	less crystal growth defects and better diffraction
higher conformational homogeneity	
more compact fold of native thermostable proteins	denser packing and enhanced diffraction
removal of mobile or unstructured appendices	
conformational stabilization by addition of natural ligands or analogs	higher crystallizability to better diffraction
crystal growth in diffusive media	superior diffraction properties

[a] Events are listed in approximate chronological order.

Crystal Properties. Overall the hierarchy of space groups in aaRS systems is similar to that observed in the PDB (Figure 4B). However, some ranking variations are observed due to the repetition in a restricted set of entries of closely related structures (e.g., in the presence of different small ligands) while retaining the same unit cell symmetry. The solvent content of aaRS/tRNA complexes tends to be slightly higher (64% on average) than for free enzymes (57% on average). This presumably reflects constraints in the arrangement of larger and less globular particles (Figure 4C). Overall, the values for aaRSs and aaRS/tRNA complexes are high when compared with globular proteins.[90] As anticipated, the resolution at which a structure is determined is correlated with the solvent content of the crystal (Figure 4C), highest resolution being frequently achieved with smallest globular aaRSs or aaRS domains. For instance, the editing domain of ThrRS (1Y2Q, 143 residues) produces densely packed crystals with extremely low solvent content (29%). Human mini-TyrRS (47% solvent) diffracts X-rays to a resolution of 1.2 Å, whereas the full-length enzyme could not yet be crystallized.[62] On the opposite, crystals of the large full-length PheRS from *T. thermophilus*[81] and of the ValRS/tRNA complex[91] which both gave structures at resolution 2.9 Å contain as much as 74 and 83% solvent, respectively. This also strongly suggests that a crystal polymorph with a lower solvent content may be the key to the success of structure determination. The structure of the AspRS/tRNA^{Asp} complex was determined using orthorhombic crystals (diffraction limit ~3 Å, solvent content 70%)[39] instead of cubic ones (diffraction limit ~7 Å, solvent content 80%),[92] and, in the case of the free AspRS, the best diffraction with respect to resolution and isotropy was also observed for the denser polymorph.[14]

Choice of the Targets. The source of the aaRS that were studied changed with the years (Figure 1A). First successes were obtained with biomolecules isolated from thermostable bacteria. Archaeal aaRSs have attracted crystal growers more recently and become a priority under the influence of structural genomics projects. The reason is that aaRSs from archaea and bacteria have a higher propensity to crystallize because their more compact structure is deprived of appended and mobile domains (Figures 2 and 3). In the case of extremophiles, nature has selected stable conformers that are functional under extreme conditions. In contrast, eukaryotic systems are under-represented due to the difficulties encountered in the preparation of pure, homogeneous, and crystallizable samples. The progress in protein purification and expression, and the rising interest for human aminoacylation systems in relation with pathologies[93] have led to a boom of new eukaryotic structures. AaRSs are ubiquitous and essential enzymes. For new drug design opportunities, it is important to perform comparative study of pathogenic versus human cytosolic or mitochondrial systems. This will probably move research more toward aaRSs from higher eukarya. In this context, thermophilic eukarya like the worm *Alvinella pompejana* are promising source of aaRSs.

4. Conclusions and Perspectives

In the past, the time span between the growth of the first aaRS crystal and the final resolution of the structure was often long because crystallization and/or crystallographic difficulties had to be overcome for the first time. It was respectively 31 and 20 years for *E. coli* apo-MetRS[7,9] and *S. cerevisiae* apo-AspRS.[6,44] In the case of yeast AspRS/tRNA^{Asp} complex, 8 years were necessary to obtain the adequate orthorhombic crystals[43] for structure determination starting from cubic crystals[35,92] which exhibited growth pathologies and gave only mediocre diffraction patterns. The continued study of the crystallization behavior of aaRS systems has revealed a puzzle of unforeseen features and inspired new interdisciplinary research lines covering biology, chemistry, material science, physical chemistry, physics and engineering. It was one of the motivations that has led to the birth of the biocrystallogenesis science covered by ICCBM meetings.[94] The increasing knowledge of aaRS properties has given clues about how to tailor their structures (e.g., to eliminate dangling domains or modify surface properties) and refine their crystallization conditions (e.g., by adding substrates, substrate analogues, or specific additives stabilizing the protein structure) for improved crystal production. Nowadays numerous approaches that were applied for the first time to aaRSs are applicable to the crystallization of proteins in general (Table 2).

Biocrystallogenesis has also benefited from pilot studies on protein models that are easily accessible to experimenters, such as the small and globular lysozyme or thaumatin (for an overview of the literature see ref 94). The continuous efforts to grow better aaRS crystals for structural biology have generated a wealth of data that are of interest for physical-chemists and specialists of crystal growth. Indeed, AaRSs provide robust and more realistic models for crystal growth than lysozyme or thaumatin. For instance, TrpRS was the test molecule used to implement the multifactorial approach for crystal growth optimization in the presence of small ligands.[31] Likewise, AspRSs served to develop novel crystallogenesis strategies like the use of phase diagram as an optimization tool.[13,95] In particular, the crystals of the AspRS from *T. thermophilus* have been shown to grow by Oswald ripening, that is, single macrocrystals nucleate in a precipitate and their growth rate is limited by the dissolution of the insoluble phase.[96] The same high-molecular weight protein was also employed in comparative crystal growth experiments in diffusive media (i.e., under microgravity, in gel, or by counter-diffusion).[95,97,98] Finally, it was used to visualize the growth mechanism by atomic force microscopy[95] and to probe intrinsic crystal quality by X-ray topography.[99]

As a final remark, this work illustrates the amount of information that can be extracted from the PDB for a given protein family or class of enzymes. Our analysis remains partial because PDB format does not or only sparsely includes

crystallization details.[89] More useful information is certainly hidden in the plethora of published or nonpublished crystallization data. Supplementary data could be extracted in combination with other resources like the Biological Macromolecule Crystallization database (BMCD)[100] and the Marseille Data Base.[101] All this will be useful to find more correlations and design novel specific sparse matrices.

Acknowledgment. This work was supported by the French Centre National de la Recherche Scientifique (CNRS), the French Ministry for Research (ACI-BCMS 042358), the Université Louis Pasteur in Strasbourg and the Association Française contre les Myopathies (AFM). E.T. was the recipient of a fellowship from the French Ministry for Research. K. Dhouib is acknowledged for her contribution to figure preparation.

References

(1) Ibba, M.; Francklyn, C.; Cusack, S. *The Aminoacyl-tRNA Synthetases*; Landes Bioscience: Georgetown, TX, 2005.
(2) Giegé, R. The early history of tRNA recognition by aminoacyl-tRNA synthetases. *J. Biosci.* **2006**, *31*, 477–488.
(3) Berman, H. M.; Westbrook, J.; Feng, Z.; Gilliland, G.; Bhat, T. N.; Weissig, H.; Shindyalov, I. N.; Bourne, P. E. The protein data bank. *Nucleic Acids Res.* **2000**, *28*, 235–242.
(4) Carter, C. W.; Carter, C. W., Jr. Protein crystallization using incomplete factorial experiments. *J. Biol. Chem.* **1979**, *254*, 12219–12223.
(5) Lagerkvist, U.; Rymo, L.; Lindquist, O.; Andersson, E. Some properties of crystals of lysine transfer ribonucleic acid ligase from yeast. *J. Biol. Chem.* **1972**, *247*, 3897–3899.
(6) Dietrich, A.; Giegé, R.; Comarmond, M.-B.; Thierry, J.-C.; Moras, D. Crystallographic studies on the aspartyl-tRNA synthetase-tRNA^{asp} system from yeast. the crystalline aminoacyl-tRNA synthetase. *J. Mol. Biol.* **1980**, *138*, 129–135.
(7) Waller, J.; Risler, J.; Monteilhet, C.; Zelwer, C. Crystallisation of trypsin-modified methionyl-tRNA synthetase from *Escherichia coli*. *FEBS Lett.* **1971**, *16*, 186–188.
(8) Jakoby, W. B. A technique for the crystallization of proteins. *Anal. Biochem.* **1968**, *26*, 295–298.
(9) Méchulam, Y.; Schmitt, E.; Maveyraud, L.; Zelwer, C.; Nureki, O.; Yokoyama, S.; Konno, M.; Blanquet, S. Crystal structure of *Escherichia coli* coli methionyl-tRNA synthetase highlights species-specific features. *J. Mol. Biol.* **1999**, *294*, 1287–1297.
(10) Serre, L.; Verdon, G.; Choinowski, T.; Hervouet, N.; Risler, J.; Zelwer, C. How methionyl-tRNA synthetase creates its amino acid recognition pocket upon L-methionine binding. *J. Mol. Biol.* **2001**, *306*, 863–876.
(11) Crépin, T.; Schmitt, E.; Méchulam, Y.; Sampson, P. B.; Vaughan, M. D.; Honek, J. F.; Blanquet, S. Use of analogues of methionine and methionyl adenylate to sample conformational changes during catalysis in *Escherichia coli* methionyl-tRNA synthetase. *J. Mol. Biol.* **2003**, *332*, 59–72.
(12) Reid, B.; Koch, G.; Boulanger, Y.; Hartley, B.; Blow, D. Crystallization and preliminary x-ray diffraction studies on tyrosyl transfer RNA synthetase from *Bacillus stearothermophilus*. *J. Mol. Biol.* **1973**, *80*, 199–201.
(13) Sauter, C.; Lorber, B.; Kern, D.; Cavarelli, J.; Moras, D.; Giegé, R. Crystallogenesis studies on aspartyl-tRNA synthetase: use of phase diagram to improve crystal quality. *Acta Crystallogr. D Biol. Crystallogr.* **1999**, *55*, 149–156.
(14) Sauter, C.; Lorber, B.; Théobald-Dietrich, A.; Giegé, R. Crystallogenesis in tRNA aminoacylation systems: how packing accounts for crystallization drawbacks with yeast aspartyl-tRNA synthetase. *J. Cryst. Growth* **2001**, *232*, 399–408.
(15) Thomas, D.; Rob, A.; Rice, D. A novel dialysis procedure for the crystallization of proteins. *Protein Eng.* **1989**, *2*, 489–491.
(16) Lee, S.; Cudney, R. A modified microdialysis button for use in protein crystallization. *J. Appl. Crystallogr.* **2004**, *37*, 504–505.
(17) Liebl, W. Genomics taken to the extreme. *Nat. Biotechnol.* **2004**, *22*, 524–525.
(18) Chernaya, M. M.; Korolev, S. V.; Reshetnikova, L. S.; Safro, M. G. Preliminary crystallographic study of the phenylalanyl-tRNA synthetase from *Thermus thermophilus* hb8. *J. Mol. Biol.* **1987**, *198*, 555–556.
(19) Reshetnikova, L.; Khodyreva, S.; Lavrik, O.; Ankilova, V.; Frolow, F.; Safro, M. Crystals of the phenylalanyl-tRNA synthetase from *Thermus thermophilus* hb8 complexed with tRNA^{phe}. *J. Mol. Biol.* **1993**, *231*, 927–929.
(20) Logan, D.; Cura, V.; Touzel, J.; Kern, D.; Moras, D. Crystallisation of the glycyl-tRNA synthetase from *Thermus thermophilus* and initial crystallographic data. *J. Mol. Biol.* **1994**, *241*, 732–735.
(21) Yaremchuk, A.; Kriklivyi, I.; Cusack, S.; Tukalo, M. Improved crystals of *Thermus thermophilus* prolyl-tRNA synthetase complexed with cognate tRNA obtained by crystallization from precipitate. *Acta Crystallogr. D Biol. Crystallogr.* **2000**, *56*, 197–199.
(22) Iwaki, J.; Suzuki, R.; Fujimoto, Z.; Momma, M.; Kuno, A.; Hasegawa, T. Overexpression, purification and crystallization of tyrosyl-tRNA synthetase from the hyperthermophilic archaeon. *Aeropyrum pernix k1*. *Acta Crystallogr. F Struct. Biol. Cryst. Commun.* **2005**, *61*, 1003–1005.
(23) Winter, G.; Hartley, B. The amino acid sequence of tryptophanyl-tRNA synthetase from *Bacillus stearothermophilus*. *FEBS Lett.* **1977**, *80*, 340–342.
(24) Kisselev, L.; Kovaleva, G. Tryptophanyl-tRNA synthethase of higher organisms: enzymological, immunochemical and cytological studies. *Sov. Sci. Rev. D. Physicochem. Biol.* **1987**, *7*, 137–186.
(25) Doublié, S.; Bricogne, G.; Gilmore, C.; Carter, C. W., Jr. Tryptophanyl-tRNA synthetase crystal structure reveals an unexpected homology to tyrosyl-tRNA synthetase. *Structure* **1995**, *3*, 17–31.
(26) Kisselev, L. L.; Favorova, O. O.; Parin, A. V.; Stel'mashchuk, V.; Kisselev, N. A. Crystallization (polymerization) of the complex of tryptophanyl-tRNA-synthetase with tryptophan. *Dokl. Akad. Nauk SSSR* **1971**, *199*, 1178–1180.
(27) Carter, C. W., Jr.; Coleman, D. E. Crystallization of substrate and product analog complexes of tryptophanyl-tRNA synthetase. *Fed. Proc.* **1984**, *43*, 2981–2983.
(28) Carter, C. W., Jr. Cloning heterologous genes into *E. coli* for enzyme production and crystal growth: problems of expression and microheterogeneity. *J. Cryst. Growth* **1988**, *90*, 168–179.
(29) Carter, C. W., Jr.; Doublié, S.; Coleman, D. E. Quantitative analysis of crystal growth. tryptophanyl-tRNA synthetase crystal polymorphism and its relationship to catalysis. *J. Mol. Biol.* **1994**, *238*, 346–365.
(30) Jancarik, J.; Kim, S. Sparse matrix sampling; a screening method for crystallization of proteins. *J. Appl. Crystallogr.* **1991**, *24*, 409–411.
(31) Carter, C. W., Jr. Response surface methods for optimizating and improving reproducibility of crystal growth. *Methods Enzymol.* **1997**, *276*, 74–99.
(32) Ilyin, V. A.; Temple, B.; Hu, M.; Li, G.; Yin, Y.; Vachette, P.; Carter, C. W. Jr. 2.9 Å crystal structure of ligand-free tryptophanyl-tRNA synthetase: domain movements fragment the adenine nucleotide binding site. *Protein Sci.* **2000**, *9*, 218–231.
(33) Giegé, R.; Lorber, B.; Ebel, J.-P.; Moras, D.; Thierry, J.-C. Cristallisation du complexe formé entre l'aspartate-tRNA de levure et son aminoacyl-tRNA synthétase spécifique. *C. R. Acad. Sc. Paris* **1980**, *D-2* (291), 393–396.
(34) Giegé, R.; Lorber, B.; Ebel, J.-P; Moras, D.; Thierry, J.-C.; Jacrot, B.; Zaccaï, G. Formation of a catalytically active complex between tRNA^{asp} and aspartyl-tRNA synthetase from yeast in high concentrations of ammonium sulphate. *Biochimie* **1982**, *64*, 357–362.
(35) Lorber, B.; Giegé, R.; Ebel, J.-P.; Berthet, C.; Thierry, J.-C.; Moras, D. Crystallization of a tRNA-aminoacyl-tRNA synthetase complex. characterization and first crystallographic data. *J. Biol. Chem.* **1983**, *258*, 8429–8435.
(36) Florentz, C.; Kern, D.; Giegé, R. Stimulatory effect of ammonium sulfate at high concentrations on the aminoacylation of tRNA and tRNA-like molecules. *FEBS Lett.* **1990**, *261*, 335–338.
(37) Dock-Bregeon, A.-C., Moras, D., Giegé, R. Nucleic acids and their complexes In *Crystallization of Nucleic Acids and Proteins. A Practical Approach*, 2nd ed.; Ducruix, A. Giegé, A., Eds.; IRL Press: Oxford, 1999, 209−243.
(38) Rould, M. A.; Perona, J. J.; Söll, D.; Steitz, T. A. Structure of e. coli glutaminyl-tRNA synthetase complexed with tRNA^{gln} and ATP at 2.8 Å resolution. *Science* **1989**, *246*, 1135–1142.
(39) Ruff, M.; Krishnaswamy, S.; Boeglin, M.; Poterszman, A.; Mitschler, A.; Podjarny, A.; Rees, B.; Thierry, J.-C.; Moras, D. Class ii aminoacyl transfer RNA synthetases: crystal structure of yeast aspartyl-tRNA synthetase complexed with tRNA^{asp}. *Science* **1991**, *252*, 1682–1689.
(40) Giegé, R.; Dock, A.-C.; Kern, D.; Lorber, B.; Thierry, J.-C.; Moras, D. The role of purification in the crystallization of proteins and nucleic acids. *J. Cryst. Growth* **1986**, *76*, 554–561.

(41) Myerson, A. *Handbook of Industrial Crystallization*, 2nd ed.; Butterworth-Heinemann: Woburn, MA, 2001.

(42) JakobyW. Crystallization as a purification technique In *Methods In Enzymology, London*; Jakoby, W., Eds.; Academic Press: New York, 1971; pp 248−252.

(43) Ruff, M.; Cavarelli, J.; Mikol, V.; Lorber, B.; Mitschler, A.; Giegé, R.; Thierry, J.-C.; Moras, D. A high resolution diffracting crystal form of the complex between yeast $tRNA^{asp}$ and aspartyl-tRNA synthetase. *J. Mol. Biol.* **1988**, *201*, 235–236.

(44) Sauter, C.; Lorber, E.; Cavarelli, J.; Moras, D.; Giegé, R. The free yeast aspartyl-tRNA synthetase differs from the $tRNA^{asp}$-complexed enzyme by structural changes in the catalytic site, hinge region, and anticodon-binding domain. *J. Mol. Biol.* **2000**, *299*, 1313–1324.

(45) Moreno, A.; Théobald-Dietrich, A.; Lorber, B.; Sauter, C.; Giegé, R. Effects of macromolecular impurities and of crystallization method on the quality of eubacterial aspartyl-tRNA synthetase crystals. *Acta Crystallogr. D Biol. Crystallogr.* **2005**, *61*, 789–792.

(46) Lorber, B., Giegé, R. Biochemical aspects and handling of macromolecular solutions and crystals. In *Crystallization of Nucleic Acids and Proteins. A Practical Approach*, 2nd ed.; Ducruix, A.,Giegé, R., Eds.; IRL Press: Oxford, 1999; pp 17−43.

(47) Mikol, V.; Vincendon, P.; Eriani, G.; Hirsch, E.; Giegé, R. Diagnostic of protein crystallization by dynamic light scattering; an application to an aminoacyl-tRNA synthetase. *J. Cryst. Growth* **1991**, *110*, 195–200.

(48) Thibault, F.; Langowski, J.; Leberman, R. Pre-nucleation crystallization studies on aminoacyl-tRNA synthetases by dynamic light-scattering. *J. Mol. Biol.* **1992**, *225*, 185–191.

(49) Abergel, C.; Rudinger-Thirion, J.; Giegé, R.; Claverie, J. Virus-encoded aminoacyl-tRNA synthetases: structural and functional characterization of mimivirus TyrRS and MetRS. *J. Virol.* **2007**, *81*, 12406–12417.

(50) Paukstelis, P. J.; Chen, J. H.; Chase, E.; Lambowitz, A. M.; Golden, B. L. Structure of a tyrosyl-tRNA synthetase splicing factor bound to a group I intron RNA. *Nature* **2008**, *451*, 94–97.

(51) Terada, T.; Nureki, O.; Ishitani, R.; Ambrogelly, A.; Ibba, M.; Soll, D.; Yokoyama, S. Functional convergence of two lysyl-tRNA synthetases with unrelated topologies. *Nat. Struct. Biol.* **2002**, *9*, 257–262.

(52) Yanagisawa, T.; Ishii, R.; Fukunaga, R.; Nureki, O.; Yokoyama, S. Crystallization and preliminary X-ray crystallographic analysis of the catalytic domain of pyrrolysyl-tRNA synthetase from the methanogenic archaeon *Methanosarcina mazei*. *Acta Crystallogr. F Struct. Biol. Cryst. Commun.* **2006**, *62*, 1031–1033.

(53) Kavran, J. M.; Gundllapalli, S.; O'Donoghue, P.; Englert, M.; Söll, D.; Steitz, T. A. Structure of pyrrolysyl-tRNA synthetase, an archaeal enzyme for genetic code innovation. *Proc. Natl. Acad. Sci. U. S. A.* **2007**, *104*, 11268–11273.

(54) Yanagisawa, T.; Ishii, R.; Fukunaga, R.; Kobayashi, T.; Sakamoto, K.; Yokoyama, S. Crystallographic studies on multiple conformational states of active-site loops in pyrrolysyl-tRNA synthetase. *J. Mol. Biol.* **2008**, *378*, 634–652.

(55) Fukunaga, R.; Yokoyama, S. Structural insights into the second step of RNA-dependent cysteine biosynthesis in archaea: crystal structure of sep-tRNA:cys-tRNA synthase from *Archaeoglobus fulgidus*. *J. Mol. Biol.* **2007**, *370*, 128–141.

(56) Kamtekar, S.; Hohn, M. J.; Park, H. S.; Schnitzbauer, M.; Sauerwald, A.; Söll, D.; Steitz, T. A. Toward understanding phosphoseryl-$tRNA^{cys}$ formation: the crystal structure of *Methanococcus maripaludis* phosphoseryl-tRNA synthetase. *Proc. Natl. Acad. Sci. U. S. A.* **2007**, *104*, 2620–2625.

(57) Dock, A.; Lorber, B.; Moras, D.; Pixa, G.; Thierry, J.-C.; Giegé, R. Crystallization of transfer ribonucleic acids. *Biochimie* **1984**, *66*, 179–201.

(58) Giegé, R., Frugier, M. Transfer RNA structure and identity In *Translation Mechanisms*; Lapointe, J., Brakier-Gringas, L.; Landes Biosciences: Georgetown, TX, 2003; p 124.

(59) Irwin, M.; Nyborg, J.; Reid, B.; Blow, D. The crystal structure of tyrosyl-transfer synthetase at 2.7 Å resolution. *J. Mol. Biol.* **1976**, *105*, 577–586.

(60) Bhat, T.; Blow, D.; Brick, P.; Nyborg, J. Tyrosyl-tRNA synthetase forms a mononucleotide-binding fold. *J. Mol. Biol.* **1982**, *158*, 699–709.

(61) Brick, P.; Bhat, T. N.; Blow, D. M. Structure of tyrosyl-tRNA synthetase refined at 2.3 Å resolution. Interaction of the enzyme with the tyrosyl adenylate intermediate. *J. Mol. Biol.* **1989**, *208*, 83–98.

(62) Yang, X.; Skene, R.; McRee, D.; Schimmel, P. Crystal structure of a human aminoacyl-tRNA synthetase cytokine. *Proc. Natl. Acad. Sci. U. S. A.* **2002**, *99*, 15369–15374.

(63) Kobayashi, T.; Sakamoto, K.; Takimura, T.; Sekine, R.; Kelly, V. P.; Kamata, K.; Nishimura, S.; Yokoyama, S. Structural basis of nonnatural amino acid recognition by an engineered aminoacyl-tRNA synthetase for genetic code expansion. *Proc. Natl. Acad. Sci. U. S. A.* **2005**, *102*, 1366–1371.

(64) Zhang, Y.; Wang, L.; Schultz, P. G.; Wilson, I. A. Crystal structures of apo wild-type *M. jannaschii* tyrosyl-tRNA synthetase (TyRS) and an engineered TyrRS specific for *o*-methyl-l-tyrosine. *Protein Sci.* **2005**, *14*, 1340–1349.

(65) Yang, X. L.; Otero, F. J.; Skene, R. J.; McRee, D. E.; Schimmel, P;. Ribas de Pouplana, L. Crystal structures that suggest late development of genetic code components for differentiating aromatic side chains. *Proc. Natl. Acad. Sci. U. S. A.* **2003**, *100*, 15376–15380.

(66) Yu, Y.; Liu, Y.; Shen, N.; Xu, X.; Xu, F.; Jia, J.; Jin, Y.; Arnold, E.; Ding, J. Crystal structure of human tryptophanyl-tRNA synthetase catalytic fragment: insights into substrate recognition, tRNA binding, and angiogenesis activity. *J. Biol. Chem.* **2004**, *279*, 8378–8388.

(67) Kise, Y.; Lee, S. W.; Park, S. G.; Fukai, S.; Sengoku, T.; Ishii, R.; Yokoyama, S.; Kim, S.; Nureki, O. A short peptide insertion crucial for angiostatic activity of human tryptophanyl-tRNA synthetase. *Nat. Struct. Mol. Biol.* **2004**, *11*, 149–156.

(68) Shen, N.; Guo, L.; Yang, B.; Jin, Y.; Ding, J. Structure of human tryptophanyl-tRNA synthetase in complex with $tRNA^{trp}$ reveals the molecular basis of tRNA recognition and specificity. *Nucleic Acids Res.* **2006**, *34*, 3246–3258.

(69) Yang, X. L.; Otero, F. J.; Ewalt, K. L.; Liu, J.; Swairjo, M. A.; Kohrer, C.; RajBhandary, U. L.; Skene, R. J.; McRee, D. E.; Schimmel, P. Two conformations of a crystalline human tRNA synthetase-tRNA complex: implications for protein synthesis. *EMBO J.* **2006**, *25*, 2919–2929.

(70) Yang, X. L.; Guo, M.; Kapoor, M.; Ewalt, K. L.; Otero, F. J.; Skene, R. J.; McRee, D. E.; Schimmel, P. Functional and crystal structure analysis of active site adaptations of a potent anti-angiogenic human tRNA synthetase. *Structure* **2007**, *15*, 793–805.

(71) Blanquet, S., Crépin, T., Mechulam, Y., Schmitt, E. Methionyl-tRNA synthetases. In *The aminoacyl-tRNA synthetases*; Ibba, M., Francklyn, C., Cusack, S., Eds.; Landes Bioscience: Georgetown, TX, 2005; pp 47−58.

(72) Belrhali, H.; Yaremchuk, A.; Tukalo, M.; Larsen, K.; Berthet-Colominas, C.; Leberman, R.; Beijer, B.; Sproat, B.; Als-Nielsen, J.; Grübel, G.; et al. Crystal structures at 2.5 angstrom resolution of seryl-tRNA synthetase complexed with two analogs of seryl adenylate. *Science* **1994**, *263*, 1432–1436.

(73) Sekine, S.; Shichiri, M.; Bernier, S.; Chênevert, R.; Lapointe, J.; Yokoyama, S. Structural bases of transfer RNA-dependent amino acid recognition and activation by glutamyl-tRNA synthetase. *Structure* **2006**, *14*, 1791–1799.

(74) Bonnefond, L.; Frugier, M.; Touzé, E.; Lorber, B.; Florentz, C.; Giegé, R.; Sauter, C.; Rudinger-Thirion, J. Crystal structure of human mitochondrial tyrosyl-tRNA synthetase reveals common and idiosyncratic features. *Structure* **2007**, *15*, 1505–1516.

(75) Dale, G. E.; Oefner, C.; D'Arcy, A. The protein as a variable in protein crystallization. *J. Struct. Biol.* **2003**, *142*, 88–97.

(76) Giegé, R.; Moras, D.; Thierry, J. Yeast transfer RNA^{asp}: a new high resolution x-ray diffracting crystal form of a transfer RNA. *J. Mol. Biol.* **1977**, *115*, 91–96.

(77) Moras, D.; Comarmond, M.-B.; Fischer, J.; Weiss, R.; Thierry, J.-C.; Ebel, J.-P.; Giegé, R. Crystal structure of yeast $tRNA^{asp}$. *Nature* **1980**, *288*, 669–674.

(78) Boeglin, M.; Dock-Bregeon, A.-C.; Eriani, G.; Gangloff, J.; Ruff, M.; Poterszman, A.; Thierry, J.-C.; Moras, D. Crystallization of *Escherichia coli* aspartyl-tRNA synthetase in its free state and in a complex with yeast $tRNA^{asp}$. *Acta Crystallogr. D Biol. Crystallogr.* **1996**, *52*, 211–214.

(79) Moulinier, L.; Eiler, S.; Eriani, G.; Gangloff, J.; Thierry, J.-C.; Gabriel, K.; McClain, W. H.; Moras, D. The structure of an asprs-tRNA(asp) complex reveals a tRNA-dependent control mechanism. *EMBO J.* **2001**, *20*, 5290–5301.

(80) Frugier, M.; Moulinier, L.; Giegé, R. A domain in the n-terminal extension of class IIb eukaryotic aminoacyl-tRNA synthetases is important for tRNA binding. *EMBO J.* **2000**, *19*, 2371–2380.

(81) Mosyak, L.; Reshetnikova, L.; Goldgur, Y.; Delarue, M.; Safro, M. Structure of phenylalanyl-tRNA synthetase from *Thermus thermophilus*. *Nat. Struct. Biol.* **1995**, *2*, 537–547.

(82) Goldgur, Y.; Mosyak, L.; Reshetnikova, L.; Ankilova, V.; Lavrik, O.; Khodyreva, S.; Safro, M. The crystal structure of phenylalanyl-tRNA synthetase from *Thermus thermophilus* complexed with cognate $tRNA^{phe}$. *Structure* **1997**, *5*, 59–68.

(83) Kim, S.; Quigley, G.; Suddath, F.; McPherson, A.; Sneden, D.; Kim, J.; Weinzierl, J.; Rich, A. Three dimensional structure of yeast phenylalanine transfer RNA. Folding of the polynucleotide chain. *Science* **1973**, *179*, 285–288.

(84) Levin, I.; Kessler, N.; Moor, N.; Klipcan, L.; Koc, E.; Templeton, P.; Spremulli, L.; Safro, M. Purification, crystallization and preliminary X-ray characterization of a human mitochondrial phenylalanyl-tRNA synthetase. *Acta Crystallogr. F Struct. Biol. Cryst. Commun.* **2007**, *63*, 761–764.

(85) Mikol, V.; Rodeau, J.-L.; Giegé, R. Changes of ph during biomacromolecule crystallization by vapor diffusion using ammonium sulfate as the precipitant. *J. Appl. Crystallogr.* **1989**, *22*, 155–161.

(86) Rodeau, J.-L.; Mikol, V.; Giegé, R.; Lutun, P. Kinetics of pH changes in the vapor diffusion method of protein crystallization using ammonium sulfate as the precipitant. *J. Appl. Crystallogr.* **1991**, *24*, 135–141.

(87) Sissler, M.; Lorber, B.; Messmer, M.; Schaller, A.; Pütz, J.; Florentz, C. Handling mammalian mitochondrial tRNAs and aminoacyl-tRNA synthetases for functional and structural characterization. *Methods* **2008**, *44*, 176–189.

(88) Lorber, B. To save crystallization data. *Acta Crystallogr. D Biol. Crystallogr.* **2001**, *57*, 479.

(89) Peat, T. S.; Christopher, J. A.; Newman, J. Tapping the protein data bank for crystallization information. *Acta Crystallogr. D Biol. Crystallogr.* **2005**, *61*, 1662–1669.

(90) Briand, C.; Poterszman, A.; Mitschler, A.; Yusupov, M.; Thierry, J.-C.; Moras, D. Crystals of *Thermus thermophilus* $tRNA^{asp}$ complexed with its cognate aspartyl-tRNA synthetase have a solvent content of 75%. comparison with other aminoacylation systems. *Acta Crystallogr. D Biol. Crystallogr.* **1998**, *54*, 1382–1386.

(91) Fukai, S.; Nureki, O.; Sekine, S.; Shimada, A.; Tao, J.; Vassylyev, D. G.; Yokoyama, S. Structural basis for double-sieve discrimination of L-valine from L-isoleucine and L-threonine by the complex of tRNA(val) and valyl-tRNA synthetase. *Cell* **2000**, *103*, 793–803.

(92) Podjarny, A.; Rees, B.; Thierry, J.-C.; Cavarelli, J.; Jésior, J.-C.; Roth, M.; Lewitt-Bentley, A.; Kahn, R.; Lorber, B.; Ebel, J.-P.; et al. Yeast tRNA(asp)-aspartyl-tRNA synthetase complex: low resolution crystal structure. *J. Biomol. Struct. Dyn.* **1987**, *5*, 187–198.

(93) Scheper, G. C.; van der Knaap, M. S.; Proud, C. G. Translation matters: protein synthesis defects in inherited disease. *Nat. Rev. Genet.* **2007**, *8*, 711–723.

(94) McPherson, A.; Giegé, R. Crystallogenesis research for biology in the last two decades as seen from the international conferences on the crystallization of biological macromolecules. *Cryst. Growth Des.* **2007**, *7*, 2126–2133.

(95) Zhu, D.-W.; Lorber, B.; Sauter, C.; Ng, J. D.; Bénas, P; Grimellec, C.; Le, C.; Giegé, R. Growth kinetics, diffraction properties and effect of agarose on the stability of a novel crystal form of *Thermus thermophilus* aspartyl-tRNA synthetase-1. *Acta Crystallogr. D Biol. Crystallogr.* **2001**, *57*, 552–558.

(96) Ng, J. D.; Lorber, B.; Witz, J.; Théobald-Dietrich, A.; Kern, D.; Giegé, R. The crystallization of macromolecules from precipitates: evidence for ostwald ripening. *J. Cryst. Growth* **1996**, *168*, 50–62.

(97) Ng, J. D.; Sauter, C.; Lorber, B.; Kirkland, N.; Arnez, J.; Giegé, R. Comparative analysis of space-grown and earth-grown crystals of an aminoacyl-tRNA synthetase: space-grown crystals are more useful for structural determination. *Acta Crystallogr. D Biol. Crystallogr.* **2002**, *58*, 645–652.

(98) Lorber, B.; Théobald-Dietrich, A.; Charron, C.; Sauter, C.; Ng, J. D.; Zhu, D.-W.; Giegé, R. From conventional crystallization to better crystals from space: a review on pilot crystallogenesis studies with aspartyl-tRNA synthetase. *Acta Crystallogr. D Biol. Crystallogr.* **2002**, *58*, 1674–1680.

(99) Lorber, B.; Sauter, C.; Ng, J. D.; Zhu, D.-W.; Giegé, R.; Vidal, O.; Robert, M.-C.; Capelle, B. Characterization of protein and virus crystals by quasi-planar wave X-ray topography: a comparison between crystals grown in solution and in agarose gel. *J. Cryst. Growth* **1999**, *204*, 357–368.

(100) Gilliland, G. L.; Tung, M.; Ladner, J. E. The biological macromolecule crystallization database: crystallization procedures and strategies. *Acta Crystallogr. D Biol. Crystallogr.* **2002**, *58*, 916–920.

(101) Charles, M.; Veesler, S.; Bonneté, F. MPCD: a new interactive online crystallization data bank for screening strategies. *Acta Crystallogr. D Biol. Crystallogr.* **2006**, *62*, 1311–1318.

CG8007766